Breimer, M. E., Hansson, G. C., Karlsson, K.-A., & Leffler, H. (1982a) *J. Biol. Chem. 257*, 557-568.
Breimer, M. E., Falk, K.-E., Hansson, G. C., & Karlsson, K.-A. (1982b) *J. Biol. Chem. 257*, 50-59.
Breimer, M. E., Hansson, G. C., Karlsson, K.-A., & Leffler, H. (1982c) *J. Biol. Chem. 257*, 906-912.
Breimer, M. E., Hansson, G. C., Karlsson, K.-A., & Leffler, H. (1982d) *Biochim. Biophys. Acta 710*, 415-427.
Hakomori, S.-i. (1984) *Annu. Rev. Immunol. 2*, 103-126.
Hallgren, P., & Lundblad, A. (1977) *J. Biol. Chem. 252*, 1014-1022.
Hansson, G. C. (1988) *Adv. Exp. Med. Biol. 228*, 465-494.
Hansson, G. C., Bouhours, J.-F., & Ångström, J. (1987) *J. Biol. Chem. 262*, 13135-13141.
Ito, M., & Yamagata, T. (1986) *J. Biol. Chem. 261*, 14278-14282.
Karlsson, H., Carlstedt, I., & Hansson, G. C. (1987) *FEBS Lett. 226*, 23-27.
Karlsson, K.-A., Pascher, I., Pimlott, W., & Samuelsson, B. E. (1974) *Biomed. Mass Spectrom. 1*, 49-56.
Kobata, A. (1972) *Methods Enzymol. 28*, 262-271.
Larson, G., Karlsson, H., Hansson, G. C., & Pimlott, W. (1987) *Carbohydr. Res. 161*, 281-290.
Li, S.-C., DeGasperi, R., Muldrey, J. E., & Li, Y.-T. (1986) *Biochem. Biophys. Res. Commun. 141*, 346-352.
Mirelman, D., Ed. (1986) *Microbial Lectins and Agglutinins*, Wiley, New York.
Nilsson, B., & Zopf, D. (1983) *Arch. Biochem. Biophys. 222*, 628-648.
Samuelsson, B., & Samuelsson, K. (1969) *J. Lipid Res. 10*, 41-46.
Simons, K., & van Meer, G. (1988) *Biochemistry 27*, 6197-6202.
Smith, E. L., McKibbin, J. M. Karlsson, K.-A., Pascher, I., & Samuelsson, B. E. (1975) *Biochemistry 14*, 2120-2124.
Sweeley, C. C., Moskal, J. R., Nunez, H., & Matsuura, F. (1980) in *Proceedings of the 27th International Congress of Pure and Applied Chemistry* (Varmavuori, A., Ed.) pp 233-244, Pergamon Press, Oxford.
Wang, W.-T., Matsuura, F., & Sweeley, C. C. (1983) *Anal. Biochem. 134*, 398-405.

Fluorescent Molecular Rotors: A New Class of Probes for Tubulin Structure and Assembly†

Chun En Kung and Juta K. Reed*
Department of Chemistry, University of Toronto, Erindale Campus, Mississauga, Ontario L5L 1C6, Canada
Received September 21, 1988; Revised Manuscript Received February 23, 1989

ABSTRACT: 9-(Dicyanovinyl)julolidine (DCVJ) is a fluorescent dye whose intramolecular rotational relaxation is solvent dependent. Since its quantum yield increases with decreasing free volume, this molecule has been very useful in monitoring synthetic polymer reactions and measuring local microviscosity changes in phospholipid bilayers [Loutfy, R. O. (1986) *Pure Appl. Chem. 58*, 1239-1248; Kung, C. E., & Reed, J. K. (1986) *Biochemistry 25*, 6114-6121]. We have used DCVJ to follow the polymerization of tubulin, a protein that can assemble into a variety of polymorphic microstructures. DCVJ binding to free tubulin is accompanied by an increase in quantum yield, indicating that DCVJ has become partially immobilized. At 4 °C, DCVJ binds to a single population of high-affinity hydrophobic sites (K_d = 1.12 ± 0.26 μM) with a stoichiometry that is protein concentration dependent. n, the number of moles of DCVJ bound per mole of $\alpha\beta$ dimer, approaches 1 at concentrations ≤0.5 mg/mL but decreases to a lower limit of ≈0.3 at concentrations ≥2.0 mg/mL. The quantum yield also increases with increasing protein concentration. This trend is unaltered by the presence of microtubule-associated proteins. These results are analyzed in terms of a concentration-dependent oligomerization of tubulin at 4 °C. When tubulin is polymerized at 37 °C to microtubules or to sheets in the presence of Zn^{2+}, the fluorescence intensity of DCVJ increases although the magnitude of this increase differs significantly. We are able to use the distinct fluorescent and binding characteristics of the bound dye to distinguish between these two polymorphs on a molecular level.

Microtubules are cylindrically ordered polymers that play a key role in the cytoskeletal architecture of all eukaryotic cells, providing form, shape, and mobility. They participate in a wide range of dynamic cellular functions including exocytosis, intracellular transport, and mitotic spindle formation to name but a few [for reviews, see Dustin (1984) and Roberts and Hyams (1979)].

The predominant protein of microtubules, comprising approximately 75-85% of the total mass, is tubulin, a heterodimer composed of two nonidentical α and β subunits, each of approximately 55 000 daltons. In addition, a number of nontubulin proteins, termed microtubule-associated proteins (MAPs),[1] are isolated with tubulin during purification and appear to play a crucial role in in vivo microtubule formation (Borisy et al., 1975).

The assembly of tubulin dimers to form complex oligomeric structures has been the subject of considerable research in a

† This work was supported by Natural Sciences and Engineering Research Council of Canada Grant A0498.
* Author to whom correspondence should be addressed.

[1] Abbreviations: MAPs, microtubule-associated proteins; MTP, microtubule protein(s); DCVJ, 9-(dicyanovinyl)julolidine; PC-tubulin, phosphocellulose-purified tubulin; Pipes, piperazine-N,N'-bis(2-ethanesulfonic acid); EGTA, ethylene glycol bis(β-aminoethyl ether)-N,N,N',N'-tetraacetic acid; DPPC, dipalmitoylphosphatidylcholine; GTP, guanosine 5′-triphosphate; SDS, sodium dodecyl sulfate.

0006-2960/89/0428-6678$01.50/0 © 1989 American Chemical Society

number of laboratories (Correia & Williams, 1983; Kirchner, 1978; Mandelkow et al., 1980). In vitro polymerization appears to be a predominantly entropy-driven process (Erickson & Pantaloni, 1981) that can be induced by a number of experimental conditions to yield a variety of polymorphic microstructures. These include not only the well-characterized 13-protofilament microtubule believed to be the predominant in vivo form but also rings, sheets, and such bizarre assemblies as hoops and helical ribbons (Burton, 1981; Mandelkow & Mandelkow, 1981; Carlier & Pantaloni, 1978; Baker & Amos, 1978; Gaskin & Kress, 1977; White et al., 1987; Eagle et al., 1983). Although many of these anomalous polymorphs do not appear to exist in normal cells, it is possible that during chemotherapeutic treatment with the anticancer alkaloids vinblastine and vincristine, nonmicrotubular structures may be present in vivo (Dustin et al., 1980).

Models to describe mechanisms of assembly of microtubules and other polymorphic structures have been proposed (Correia & Williams, 1983). While there is considerable debate as to the sequence of specific events (prenucleation, nucleation, etc.) and the nature of the aggregates occurring at each stage (Spann et al., 1987; Mandelkow et al., 1983; Kirschner, 1978; Bordas et al., 1983), it is fairly clear that longitudinal interactions between $\alpha\beta$ dimers yield protofilaments of varying length while lateral associations between protofilaments yield the more complex supramolecular assemblies. What is not known for certain is the nature of these interactions although most of the data support both ionic and hydrophobic interactions.

In vitro polymerization of tubulin is normally monitored by turbidimetric changes (Gaskin et al., 1974). The increase in absorbance, usually at 350 nm, is roughly proportional to the total mass of the polymer. Although this method adequately represents a measure of the weight average of the degree of polymerization, it does not distinguish between the many kinds of polymorphic aggregates that have been identified by electron microscopy and X-ray diffraction analysis. Furthermore, the shape of the scatterer also determines the magnitude of the turbidity (Correia & Williams, 1983; Gaskin et al., 1974).

Fluorescence spectroscopy has been widely used to study conformational dynamics of many proteins and complex molecular assemblies although to date this approach has seen limited use in the study of tubulin polymerization. Bis(1,8-anilinonaphthalenesulfonate) (Horowitz et al., 1984) binds to tubulin and inhibits polymerization while 4′,6-diamidino-2-phenylindole (Bonne et al., 1985) binds but does not change its fluorescence properties with polymerization although the binding affinity is increased. These molecules report primarily on the dielectric constant of their environment, and this property appears to be relatively unchanged during assembly.

We have been studying a new group of fluorophores referred to as molecular rotors. These molecules are characterized by a charge-transfer excited singlet state which can rapidly deactivate through internal rotation about the donor–acceptor bond. In a highly constrained environment such as a solvent of high viscosity, the predominant decay pathway is radiative, and one observes a large increase in the fluorescence quantum yield. We have studied the properties of one of these molecules called 9-(dicyanovinyl)julolidine (DCVJ) in phospholipid bilayers and detergent micelles (Kung & Reed, 1986) and have shown that the fluorescence quantum yield is governed by the solvent (or hydrocarbon) free volume as predicted by the Förster–Hoffmann expression.

In this paper, we report on the fluorescence properties of DCVJ in tubulin and polymerized tubulin assemblies. These studies show not only that DCVJ binds to tubulin with a high affinity but also that the fluorescence properties change upon polymerization.

Materials and Methods

Instrumentation. Fluorescence measurements were recorded on an SLM 4800 series spectrofluorometer coupled to a PC-XT computer. The excitation was usually at 430 nm. Fluorescence quantum yields were calculated from a comparison of the integrated corrected emission spectra with a GG21 standard block (Hellma, $\Phi = 0.494$) as a reference. For DCVJ binding studies with tubulin preparations at 4 and 37 °C, the fluorescence intensities were recorded at 495 and 498 nm, respectively, and corrected for inner filter effects according to the method outlined by Lakowicz (1983). A thermostated sample holder was used, and all temperatures were monitored with a thermocouple. Absorbance spectra were recorded with a Beckman DU-50 spectrophotometer.

Preparation of Tubulin. Microtubule proteins (MTP), 3× cycled, were isolated from fresh bovine brains by using the assembly–disassembly procedure described by Murphy (1982). Tubulin was separated from microtubule-associated proteins by phosphocellulose (PC) column chromatography using Whatman P11 (Williams & Detrich, 1979). The elution buffer was 0.1 M Pipes, pH 6.6, 0.1 mM GTP, 1 mM EGTA, and 1 mM $MgCl_2$. The tubulin prepared by using this method was judged to be greater than 95% pure on the basis of overloaded SDS–polyacrylamide 7.5% gels. The microtubule proteins and purified tubulin (PC-tubulin) were rapidly frozen in liquid nitrogen and stored in small aliquots at −77 °C. Protein concentrations were determined by the Lowry method using bovine serum albumin as a standard (Lowry et al., 1951).

Fluorophore Binding Assays. The solutions used in all fluorophore binding studies and polymerization reactions contained 0.1 M Pipes, pH 6.6, 1 mM EGTA, 1 mM GTP, and 1 mM $MgCl_2$. Stock solutions of DCVJ were made in dry ethanol and standardized by using an extinction coefficient of 65.9×10^3 M^{-1} cm^{-1} at 453 nm. Proteins were incubated with the dye (added in microliter amounts) usually for 20 min when the binding was determined at 4 °C or for 10 min at 37 °C to ensure equilibration. The fluorescence intensity reached a constant level within this time period.

Quantitation of the dye binding parameters was made as follows. For each separate concentration of tubulin used to generate the Scatchard plots, the apparent quantum yield of the dye was determined independently. To do this, the quantum yield per micromolar bound dye was measured at three separate and low concentrations (<0.5 μM) of fluorophore, chosen such that >95% of the dye was bound to the protein. Over this dye concentration range, the protein concentration was in excess, and the fluorescence intensity was therefore directly proportional to the amount of fluorophore added, indicating that virtually all of the dye was bound. This calculated fluorescence value per micromolar dye was then used to determine the amount of dye bound for each successive dye concentration, and the concentration of free dye was estimated accordingly. It was necessary to determine a fluorescence intensity per micromolar dye bound for each tubulin concentration because it was found, as discussed below, that the quantum yield was dependent on the protein concentration. Scatchard parameters were determined by using a computer fit of the data with LIGAND-PC (Munson & Robbard, 1980).

Formation of Tubulin Polymers. The formation of tubulin sheets and microtubules was monitored by absorbance changes at 350 nm. All polymerization reactions were carried out at

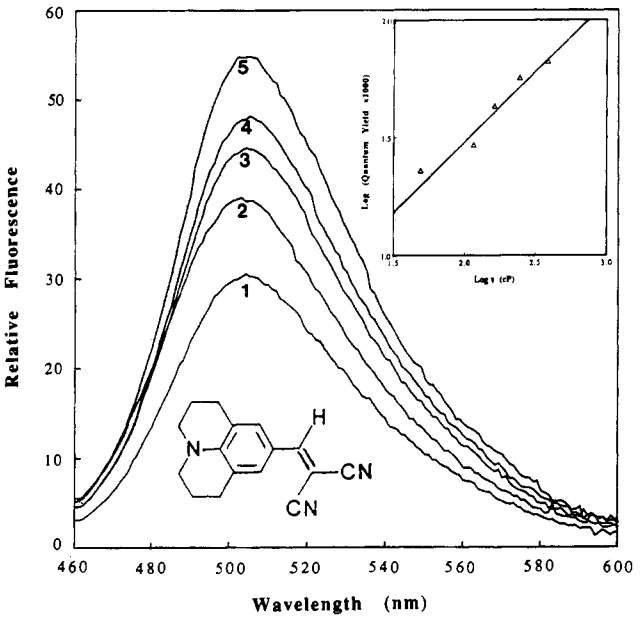

FIGURE 1: Corrected fluorescence emission spectra of 4.5 μM DCVJ in ethylene glycol/glycerol (v/v) mixtures of varying viscosity at 25 °C: (1) 7:3, η = 49 cP; (2) 5:5, η = 115 cP; (3) 4:6, η = 163 cP; (4) 3:7, η = 245 cP; (5) 2:8, η = 391 cP. The excitation wavelength was 430 nm. The inset shows the linear relationship between quantum yield (Φ_F) and viscosity (η) according to the Förster–Hoffmann expression (Förster & Hoffmann, 1971).

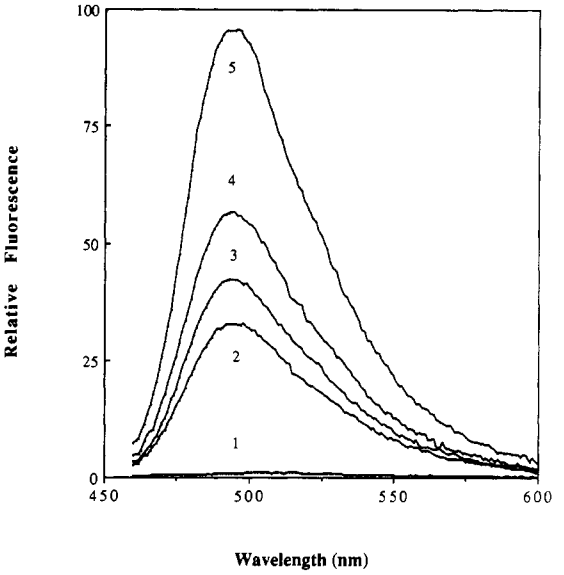

FIGURE 2: Corrected fluorescence emission spectra of DCVJ in the presence of increasing concentrations of PC-tubulin at 4 °C: (1) no tubulin; (2) 0.65 mg/mL tubulin; (3) 0.9 mg/mL tubulin; (4) 1.5 mg/mL tubulin; (5) 2.5 mg/mL tubulin. The concentration of DCVJ was 0.12 μM except in (1) where it was 0.45 μM to illustrate that in absence of protein, the fluorescence intensity of DCVJ in aqueous solution is hardly detectable.

37 °C. For Zn^{2+}-induced sheet formation, the procedure of Gaskin and Kress (1977) was routinely used.

Materials. 9-(Dicyanovinyl)julolidine (DCVJ) was prepared by the method of Kuder et al. (1977). Pipes and GTP were obtained from Sigma Chemical Co. "Super Dry" ethanol was prepared by fractional distillation of absolute ethanol and stored over 3-Å molecular sieves. All other reagents were of analytical grade.

Results

Fluorescence Characteristics of Tubulin-Bound DCVJ. DCVJ, whose structure is shown in Figure 1, absorbs maximally in the blue region of the spectrum (≈450 nm), characteristic of a π,π^* charge-transfer transition. The fluorescence emission in solvents of low viscosity is generally weak. Like other charge-transfer excited-state molecules, DCVJ has a wavelength emission maximum that is dependent on the dielectric constant of the solvent. The emission maximum ranges from 505 nm in solvents of high dielectric constant such as glycerol to approximately 480 nm in benzene which has a dielectric constant of 2. However, unlike the vast majority of the more commonly used fluorophores such as aminonaphthalenes whose fluorescence increases with decreasing dielectric constant, the fluorescence quantum yield of DCVJ is dependent rather on the solvent viscosity or, more explicitly, on the restriction placed on the rotation about the donor–acceptor bond. Figure 1 shows the emission spectra of DCVJ in mixtures of ethylene glycol/glycerol of varying viscosity. The dielectric constant is virtually unchanged. As the viscosity increases, the fluorescence quantum yield, Φ_F, increases in accordance with the Förster–Hoffmann expression (Förster & Hoffmann, 1971):

$$\log \Phi_F = C + x(\log \eta) \quad (1)$$

where η is the viscosity, C is a constant, and x is a free volume term that depends on the structural parameters of the fluorophore and represents the fraction of the total critical free volume for solvent motion that is required by the fluorophore in order to undergo torsional rearrangement.

The fluorescence spectra of DCVJ in aqueous solutions of tubulin are shown in Figure 2. The fluorescence intensity of DCVJ in aqueous buffer is extremely low as would be expected for completely unrestricted torsional rotation of the fluorophore. In the presence of PC-tubulin, the fluorescence intensity increases dramatically with increasing concentrations of protein, suggesting that the dye is bound to tubulin and that its binding reduces substantially the rotational freedom of the dye. The emission maximum of DCVJ in PC-tubulin is at 495 nm. The dielectric constant of this site can be estimated by comparison with emission maxima of the dye in other solvents and is approximately 22, slightly higher than that found for the dye in, for example, dipalmitoylphosphatidylcholine bilayers (17.9) (Kung & Reed, 1986). This would place the dye in a fairly hydrophobic environment within the tubulin molecule.

Binding of DCVJ to Tubulin at 4 °C. Preliminary DCVJ binding studies with PC-tubulin showed that DCVJ bound with a high affinity. Furthermore, there was evidence that the binding was dependent on the protein concentration. Because of this, it was not possible to use the double-titration method originally elaborated by Wang and Edelman (1971) and described in detail by Horowitz and Criscimagna (1985) to quantitate the amount of fluorophore bound to the protein at successive concentrations of fluorophore. Instead, the procedure described under Materials and Methods was found to be suitable for DCVJ binding to tubulin.

Figure 3 shows the Scatchard plots of the binding of DCVJ to PC-tubulin at tubulin concentrations ranging from 0.45 to 1.5 mg/mL at 4 °C. Under these conditions, PC-tubulin is believed to be in the unpolymerized state. In all cases even up to 2.5 mg/mL (data not shown), the plots were linear, indicating that DCVJ was bound to a single population of binding sites. The K_d (1.12 ± 0.26 μM) was also constant over this concentration range (0.45–2.5 mg/mL). On the other hand, the apparent number of binding sites, n, where n equals the number of moles of DCVJ bound per mole of tubulin dimer, decreases from 0.8–0.9 at low protein concentrations to nearly 0.3 at the highest protein concentrations studied.

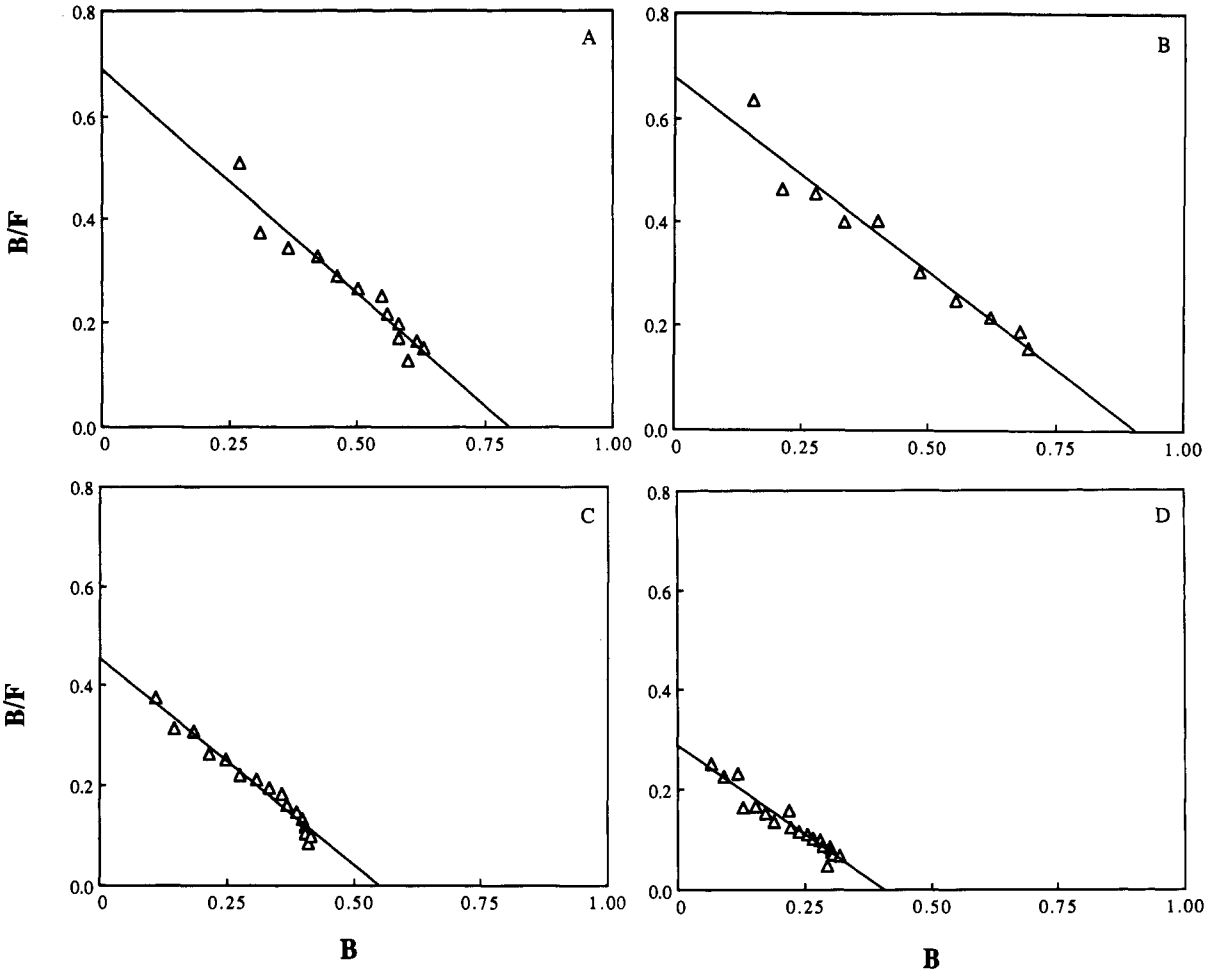

FIGURE 3: Scatchard plots for the binding of DCVJ to PC-tubulin of varying concentrations at 4 °C: (A) 0.45 mg/mL tubulin; (B) 0.55 mg/mL tubulin; (C) 0.90 mg/mL tubulin; (D) 1.5 mg/mL tubulin. *B* denotes bound DCVJ in moles per mole of tubulin dimer (110 000 daltons), and *F* denotes the concentration of free DCVJ in micromolar.

The apparent decrease in DCVJ binding stoichiometry with increasing PC-tubulin concentration is shown more clearly in Figure 4A. This plot shows that n approaches limiting values at high and low protein concentrations.

It was also found that the fluorescence intensity per micromolar bound dye increases with increasing protein concentrations. Figure 4B shows the dependence of the fluorescence quantum yield (Φ_F) of the tubulin-bound dye on the protein concentration. There appears to be a lower limit of Φ_F at low protein concentrations.

These observations may be explained if PC-tubulin was capable of concentration-dependent self-association at 4 °C. Such higher order structures or oligomers may differ morphologically and thus yield different fluorescent dye binding characteristics. In particular, the higher quantum yield experienced by the dye with increasing protein concentrations suggests a more rotationally restrictive environment.

It has been shown from near-UV CD studies that the method of tubulin isolation and possibly the removal of microtubule-associated proteins can affect the tubulin conformation (Clark et al., 1981). It is possible that the concentration dependence of the DCVJ fluorescence is a consequence of these differences and is a property of only PC-purified tubulin. To test this, the binding properties of DCVJ were determined for 3×-cycled microtubule protein preparations which contain microtubule-associated proteins. These results are summarized in Table I.

A comparison of PC-tubulin to microtubule protein (MTP) at equivalent protein concentrations shows clearly that there is no significant difference between these two preparations with respect to the dissociation constant (K_d = 0.92 ± 0.13 μM; 0.5–2.0 mg/mL). Furthermore, the binding stoichiometry observed for MTP follows the same concentration-dependent profile found for PC-tubulin. These results suggest that the fluorophore binding parameters at 4 °C are independent of the presence of the microtubule-associated proteins.

Table I: Effect of Tubulin Preparation on DCVJ Binding at 4 °C

sample	[protein] (mg/mL)	K_d (μM)[a]	n[a]
PC-tubulin	0.5	1.13	0.85
MTP[b]	0.5	0.84	0.98
PC-tubulin	1.0	0.92	0.57
PC-tubulin	2.0	0.90	0.39
MTP[b]	2.0	0.80	0.27

[a] Estimated error for the determination of K_d and n is approximately 11%. [b] MTP refers to 3×-cycled microtubule protein.

Effect of Tubulin Polymerization on DCVJ Fluorescence Properties. The results reported above were all obtained under conditions (4 °C) where tubulin is unpolymerized. It was of interest to determine whether microtubule formation or Zn^{2+}-induced sheet formation altered the structure of the DCVJ binding site in tubulin. Figure 5 shows the polymerization of PC-tubulin and microtubule protein into sheet structures and the formation of microtubules from MTP at 37 °C. In all cases, assembly was monitored turbidimetrically at 350 nm. Under all three polymerization conditions, we observe an increase in DCVJ fluorescence with time. Furthermore, under conditions of sheet formation induced by Zn^{2+},

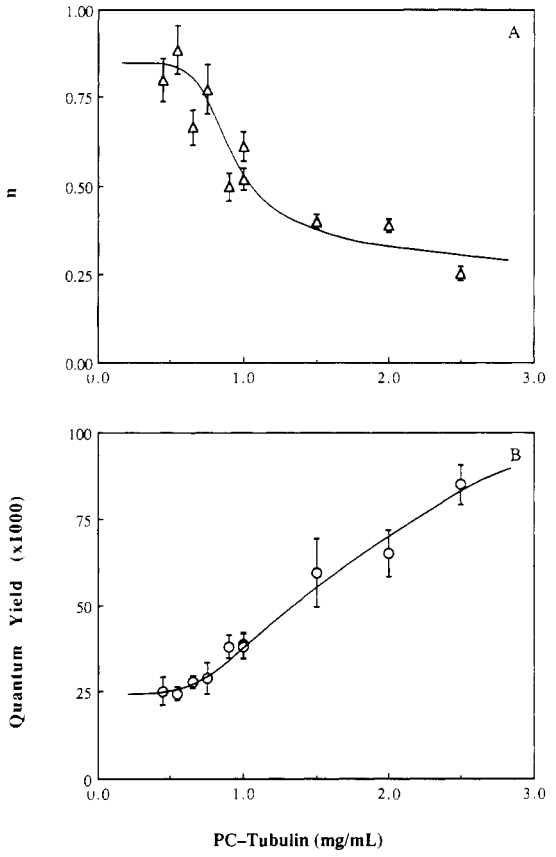

FIGURE 4: Dependence of the number of DCVJ binding sites, n (A), and the quantum yield, Φ_F (B), on the concentration of PC-tubulin at 4 °C. Values of n were calculated from Scatchard analyses and are given in moles of DCVJ per mole of tubulin dimer. Φ_F values were calculated as described under Materials and Methods.

the fluorescence profiles coincided well with the light-scattering profiles. However, the profile for fluorescence increase observed during microtubule formation is significantly different from the light-scattering profile. In addition, the fluorescence enhancement upon assembly to sheets was much greater than that observed for microtubule formation.

These results may suggest that assembly of tubulin to higher order microstructures induces a conformational change in the region of the DCVJ binding site so as to restrict the rotational mobility of the dye. In addition, the difference in the observed fluorescence changes between sheets and microtubules points to significant differences in the morphology of these two aggregates at the molecular level.

The fluorescence increase upon assembly may have resulted from an increase in the number of binding sites, a decrease in the dissociation constant, or an increase in the quantum yield. To ascertain which of these factors is responsible for this observed effect, these three parameters were determined at 37 °C following polymerization of tubulin and compared to those parameters determined at 4 °C for unpolymerized proteins. The results are shown in Table II.

For PC-tubulin, both the K_d and the dye binding stoichiometry, n, show a temperature-dependent increase. A similar increase in these binding parameters is observed for MTP going from the unpolymerized (4 °C) to the polymerized (37 °C) state. In both cases, it appears that increasing temperature exposes new dye binding sites although this trend is more pronounced for PC-tubulin than MTP. In fact, it was found that for higher concentrations of PC-tubulin at 37 °C, there appears to be a substantial increase in the amount of nonspecific binding which masks the high-affinity binding of the dye (unpublished observations). Therefore, the presence of microtubule-associated proteins appears to confer significant

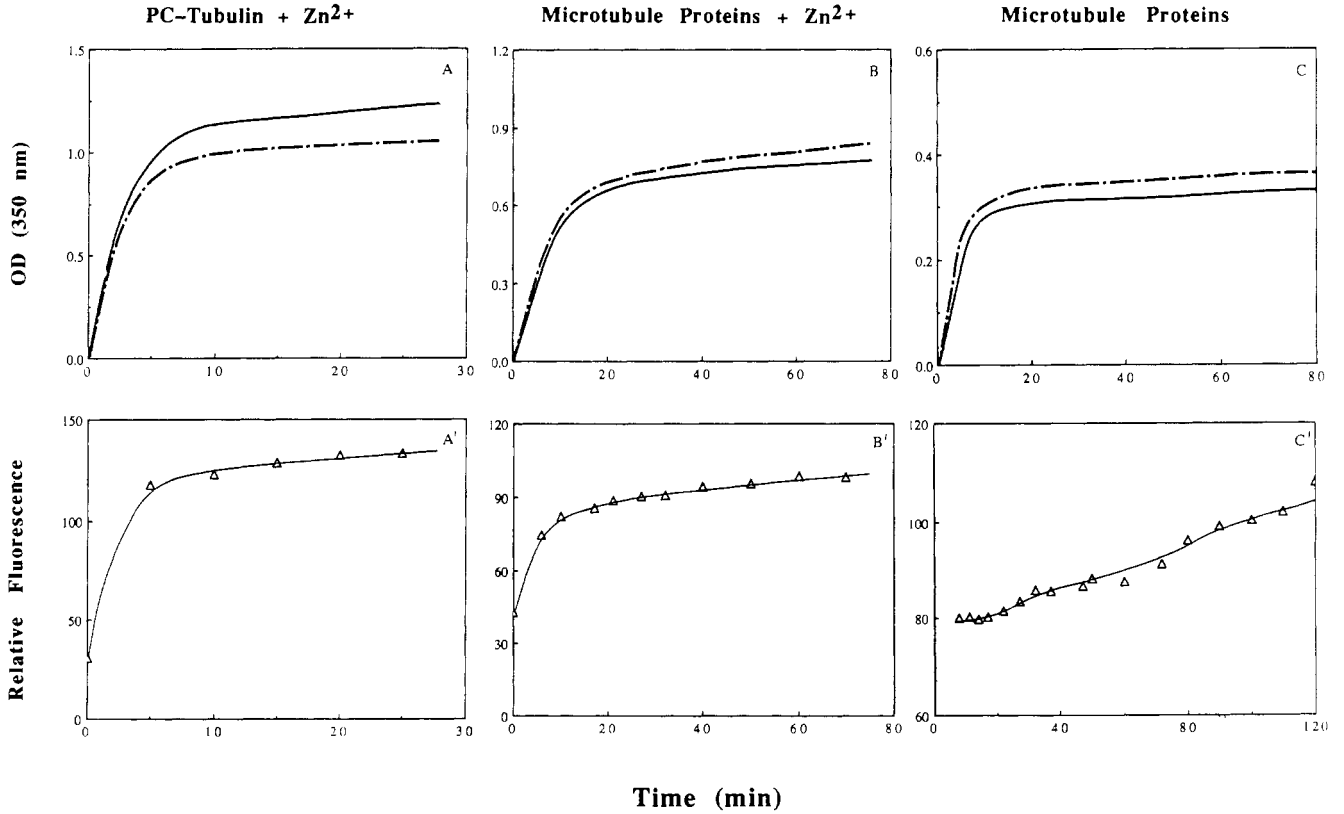

FIGURE 5: Effect of Zn^{2+} and MAPs on the polymerization of tubulin at 37 °C as monitored by DCVJ fluorescence and light scattering. The following conditions were studied: (A) Zn^{2+} (2 mM) + PC-tubulin (1 mg/mL); (B) Zn^{2+} (2 mM) + MTP (1 mg/mL); (C) MTP (2 mg/mL). The concentration of DCVJ used was 1 μM except for (C) where it was 1.3 μM. The fluorescence emission was monitored at 498 nm (A′, B′, C′). Turbidimetric measurements were made at 350 nm (A, B, C). (—) Plus DCVJ; (-·-) no DCVJ.

Table II: Temperature Dependence of DCVJ Binding Parameters to Polymerized and Unpolymerized Tubulin

sample	[protein] (mg/mL)	poly-mers[a]	temp (°C)	K_d[b] (μM)	n[b]
PC-tubulin	0.5	no	4	1.13	0.85
	0.5	no	37	2.2	2.0
MTP[c]	2.0	no	4	0.80	0.27
	2.0	yes	37	3.5	0.90
PC-tubulin + Zn^{2+}	1.0	no	4	0.74	0.27
	1.0	yes	37	0.89	0.31
MTP[c] + Zn^{2+}	1.0	no	4	0.75	0.45
	1.0	yes	37	0.85	0.33

[a] Polymerization reactions were carried out at 37 °C for approximately 70 min prior to binding analysis. [b] Estimated error for the determination of K_d and n is approximately 11%. [c] MTP refers to 3×-cycled microtubule protein.

protection to tubulin against temperature-dependent structural changes.

The observed increase in fluorescence intensity during microtubule formation (Figure 5) can now be explained as an increase in only the quantum yield. Although the binding stoichiometry increases from 0.27 to 0.90 upon polymerization, the K_d also increases from 0.8 to 3.5 μM. It can be shown, from the appropriate binding equations, that at 1 μM dye and 2 mg/mL protein, the amount of dye-bound tubulin at 37 °C is only 4% greater than that at 4 °C.

On the other hand, in the presence of Zn^{2+}, no change in K_d or dye binding stoichiometry was observed at 4 or 37 °C, and therefore the increase in fluorescence intensity upon polymerization to sheet structures is also due solely to an increase in the quantum yield.

The difference in fluorescence intensity between microtubule and sheet microstructures is shown more clearly in Figure 6. In this experiment, the MTP was allowed to polymerize at 37 °C. The initial rapid decrease in fluorescence intensity as the solution is warmed from 4 to 37 °C is due to the increased torsional rotation of the dye brought about by an increase in the available free volume. This effect would be a result of the thermally enhanced molecular freedom within the binding site. As the MTP polymerizes, there is only a small increase in fluorescence intensity. On the other hand, the addition of Zn^{2+} causes a rapid and large increase in fluorescence intensity coincident with the transition from microtubules to sheets. These observations suggest that the dye binding sites in Zn^{2+}-induced sheets are considerably more rotationally restricted than those in microtubules.

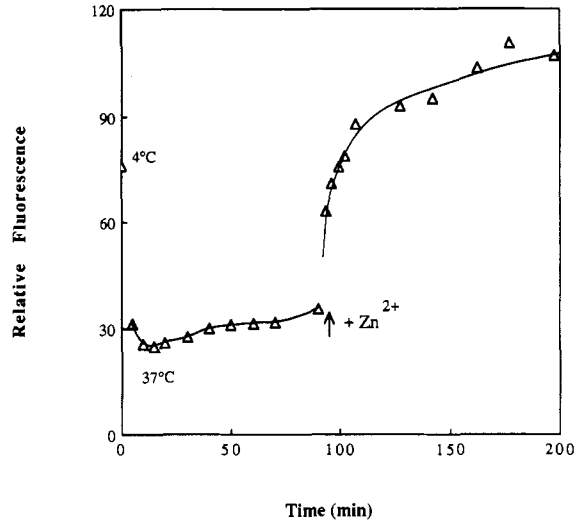

FIGURE 6: Transition of microtubules to Zn^{2+}-induced sheets at 37 °C as detected by changes in DCVJ fluorescence. [MTP] is at 2 mg/mL, and [DCVJ] is at 3 μM. The system was allowed to form microtubules prior to the addition of 3 mM Zn^{2+} (at the arrow). The fluorescence emission was monitored at 498 nm.

Discussion

Tubulin is unique among structural proteins in its ability to assemble into a wide array of ordered microstructures. This assembly is determined by such environmental factors as temperature, pH, metal cations, polyvalent cations, nucleotides, and many pharmacologically active agents. Only one of these structures namely, microtubules, is believed to be the physiologically active form, and yet, many other polymorphs can be easily generated in vitro and observed by electron microscopy and X-ray diffraction analysis. Clearly, it is the intrinsic structure of tubulin itself which determines the nature of the polymers. Nevertheless, we know very little about the molecular interactions, both ionic and hydrophobic that are provided by individual amino acids.

Fluorescent probes have been useful tools to study localized conformational changes that occur in proteins. The fluorescence intensity and emission wavelength of most probes are usually highly sensitive measures of the hydrophobicity of the dye binding site. For example, bis(1,8-anilinonaphthalenesulfonate) has been shown to bind tightly ($K_d \approx 2$ μM) to hydrophobic sites in tubulin. This dye has also been useful to study structural changes that occur in tubulin during temperature-dependent decay (Horowitz et al., 1984). Recently, a fluorescent DNA intercalator (4′,6-diamidino-2-phenylindole) has been used to monitor microtubule assembly (Bonne et al., 1985).

It cannot always be expected that protein conformational changes will necessarily lead to changes in the dielectric constant of the fluorophore binding site. Therefore, probes whose fluorescence is entirely dependent on the dielectric properties of their environment will be of little use in such cases.

Molecules such as DCVJ are one of a group of potentially useful fluorophores whose quantum yield is dependent not on the dielectric constant but rather on the rotational relaxation of the molecule itself. For these molecules, any process which restricts the relaxation pathway will result in an increase in the fluorescence intensity (Loutfy, 1981, 1986; Loutfy & Law, 1980).

Colchicine is a well-characterized antimitotic drug whose binding to tubulin leads to an enhancement in its fluorescence intensity (Bhattacharya & Wolff, 1974). Recent studies by Bhattacharya and Wolff (1984) have shown that this fluorescence increase is due primarily to the immobilization of the drug upon binding and not to changes in the dielectric constant. Thus, in this respect, colchicine and DCVJ have similar photophysical properties. In this study, we have exploited this unique characteristic of DCVJ to analyze possible molecular interactions that accompany tubulin assembly into different types of polymers.

At 4 °C, where tubulin is unpolymerized, DCVJ binds to both 3×-cycled microtubule proteins and PC-tubulin with a binding affinity of approximately 1 μM. The observed increase in fluorescence intensity upon binding reflects a partial immobilization of the dye within the binding site. In addition, the shift in emission maximum from 505 nm in aqueous buffer to 495 nm suggests that the binding site is hydrophobic. Removal of the MAPs from tubulin by ion-exchange chromatography does not appear to significantly alter the K_d or the emission maximum. The binding stoichiometry n has the same protein concentration dependence irrespective of the method of tubulin preparation. Although there is a decrease

in the number of available binding sites with increasing protein concentration, the dissociation constant appears to be relatively unaffected. We believe that this change in binding stoichiometry may be a consequence of a concentration-dependent oligomerization of tubulin at 4 °C, a process which has been described by a number of laboratories (Marcum & Borisy, 1978; Kravit et al., 1984; Correia & Williams, 1985; Spann et al., 1987).

It is well established from ultracentrifugation analysis that cold-stable oligomers (18 S to 30 S) of tubulin are present in equilibrium with the $\alpha\beta$ tubulin dimer (6 S) (Vallee & Borisy, 1978; Detrich & Williams, 1978; Frigon & Timasheff, 1975). The distribution of oligomers has been shown to be highly protein concentration dependent. More recently, this self-association of tubulin has been studied by using ultrafiltration and nondenaturing polyacrylamide gel electrophoresis by Kravit et al. (1984) and Corriea and Williams (1985), respectively, who showed the existence of a family of oligomeric tubulin species with molecular weights as high as ≈770 000. Furthermore, this self-association was found to be protein concentration dependent and to occur even in the presence of microtubule-associated proteins. One of the main contributions of MAPs appears to be their ability to stabilize the formation of single- and double-ring structures which are major components of microtubule proteins at 4 °C (Murphy & Borisy, 1975).

The decrease in DCVJ binding stoichiometry that we observe with increasing protein concentrations can now be explained if the self-association of tubulin to oligomeric structures occurs in such a manner as to mask accessible DCVJ binding sites. The observed fractional value of n can be viewed as a weighted average of the dye binding stoichiometries for a heterogeneous family of oligomers which exists in equilibrium. This effect might be a consequence of hydrophobic interactions between tubulin subunits and appears to be independent of the presence of microtubule-associated proteins. The fact that the quantum yield of the bound dye increases with increasing protein concentrations implies that the remaining accessible sites in the higher order oligomers have been structurally altered in such a way so as to reduce the free volume experienced by DCVJ. This also implies that the free tubulin dimers (low quantum yield) may not necessarily have the same three-dimensional structure as dimers in the oligomers (high quantum yield). Since the K_d is relatively unaffected, the chemical nature of the binding site remains essentially unchanged, and it is only its physical dimension or geometry that is altered. Over the protein concentration range studied, the bound dye does not appear to affect the equilibria between oligomeric species since the K_d remained unaffected.

Tubulin is known to possess two guanine nucleotide binding sites, each characterized by a distinct exchange rate. The guanine nucleotide GTP in the exchangeable site (E site) of assembled microtubules before hydrolysis exchanges readily with free GTP. However, after being hydrolyzed to GDP, GDP appears to be "locked on", and it has been suggested that this site becomes buried in the microtubule through a conformational change in tubulin (Corriea & Williams, 1983). The decrease in the DCVJ binding sites in tubulin upon oligomer formation at 4 °C may represent an analogous aggregation-induced conformational change.

The change in the physical dimensions of the dye binding site does not need to be very large to significantly reduce the torsional motion of the dye. The orientational relaxation time, $k_{or.}$, of DCVJ can be calculated from the fluorescence quantum yields (Loutfy & Arnold, 1982). At 4 °C, where $n \approx 1$ at low tubulin concentrations, the $k_{or.}$ is approximately 1.1×10^{10} s^{-1} but decreases to 3×10^9 s^{-1} at 2.5 mg/mL. For comparison, the $k_{or.}$ of DCVJ in DPPC vesicles at 4 °C (gel state) is 7.6×10^9 s^{-1} (Kung & Reed, 1986). The free volume term, x from eq 1, also provides some insight into the geometric constraints experienced by DCVJ. The term can be calculated from a plot of log $\tau_{or.}$ versus log (η/T) according to Loutfy and Arnold (1982) where $\tau_{or.} = 1/k_{or.}$. From such a plot for PC-tubulin (data not shown), x has a value of 0.59. This value is larger than that determined for DPPC vesicles in the gel or liquid-crystalline state (x = 0.52 and 0.39, respectively) (Kung & Reed, 1986). Since x reflects the fraction of the free volume needed to permit torsional relaxation, the higher fraction found for tubulin means that the three-dimensional structure of the dye binding site formed from the protein backbone imposes a higher degree of constraint on the orientational motions of DCVJ as compared to the ordered hydrocarbon matrix of DPPC bilayers. This conclusion is further supported by the observation that the activation energies for the torsional relaxation of DCVJ in PC-tubulin are much larger than those calculated for DPPC vesicles (14–15 versus 1–3 kcal/mol) (unpublished results).

The fluorescence of tubulin-bound DCVJ increases during polymerization at 37 °C to form microtubules and Zn^{2+}-induced sheets. There is a small shift in the emission wavelength from 495 to 498 nm, indicating that the dye binding site in both of these polymers may be slightly more polar than that of the unpolymerized protein at 4 °C. At the concentrations of dye used in these studies (substoichiometric), DCVJ does not appear to alter the polymerization process, as measured by the accompanying light-scattering changes.

We have also shown from Scatchard analyses of the resulting polymers at 37 °C that this increase in fluorescence intensity is a consequence of an increase in quantum yield. Therefore, those interactions between tubulin subunits which are responsible for stabilizing both microtubules and Zn^{2+}-induced sheets also bring about an additional structural perturbation within the dye binding domain of tubulin to further restrict the rotational freedom of the dye.

The polymerization of tubulin involves longitudinal association of repeating $\alpha\beta$ subunits oriented head to tail to form linear protofilaments of varying lengths. Lateral interactions between filaments lead to more complex structures such as microtubules and planar sheets that can be monitored in solution by light-scattering changes and visualized by electron microscopy. Microtubules and Zn^{2+}-induced sheets are structurally distinct polymorphs. Three-dimensional image reconstruction from electron microscopy and X-ray diffraction analyses has revealed significant differences with respect to protofilament spacing and polarity. Microtubules are composed of protofilaments aligned in parallel while Zn^{2+}-induced sheets are formed from lateral interactions between antiparallel protofilaments (Murphy & Borisy, 1972; Baker & Amos, 1978; Schultheiss & Mandelkow, 1983; Ceska & Edelstein, 1984). One consequence of this orientation is a reduction of the protofilament–protofilament spacing by 2.5 Å (50.7 to 48.2 Å) in going from microtubules to Zn^{2+}-induced sheets (with MAPs). Removal of MAPs from Zn^{2+}-induced sheets leads to a further 2-Å reduction in the spacing (McEwen et al., 1983).

In the antiparallel or inverted arrangement, the lateral subunit–subunit contacts appear to be different from those which exist between protofilaments aligned in parallel (Tamm et al., 1979). We believe that the observed increase in the quantum yield of the dye bound to Zn^{2+}-induced sheets as

compared to microtubules is primarily a result of the differences in the lateral contact sites. The MAPs' binding domain in both microtubules and sheets appears to be situated on the surface and not between neighboring protofilaments. Therefore, removal of MAPs from Zn^{2+}-induced sheets would not be expected to alter the quantum yield of the dye. Furthermore, binding studies (Table II) on Zn^{2+}-induced sheets (with and without MAPs) show no difference in either the K_d or the binding stoichiometry. Therefore, MAPs appear to have a minimal effect on the DCVJ binding site in Zn^{2+}-induced sheets.

A comparison of dye binding parameters at 37 °C between sheets and microtubules reveals interesting differences. In microtubules, the binding stoichiometry is 0.9 mol of DCVJ/dimer but is reduced to nearly 0.3 mol of DCVJ/dimer in sheets. This would be expected if the different lateral interactions between protofilaments lead to a diminished accessibility of the dye binding site. The 4-fold increase in the apparent K_d for microtubules as compared to sheets is probably a reflection of a more exposed binding site in microtubules.

Our results suggest a possible location on the polymer for the DCVJ binding site in the region near the interprotofilament contact domain. DCVJ does not affect the hydrolysis of GTP when vinblastine is either present or absent at 37 °C, indicating that the GTP binding site(s) is (are) distinct from the DCVJ binding site. In addition, neither colchicine nor vinblastine appears to affect the binding of DCVJ.

These studies with tubulin show that DCVJ can monitor molecular events that accompany protein concentration dependent oligomer formation at 4 °C and polymerization processes that occur at 37 °C. Although these two modes of self-assembly may be very similar in the presence of Zn^{2+}, they can be clearly distinguished in the absence of Zn^{2+} on the basis of the dye binding properties. It is noteworthy that although light scattering and DCVJ fluorescence are coincident during Zn^{2+}-induced sheet formation, they follow different time courses during microtubule formation (see Figure 5C). It is possible that this gradual increase in the fluorescence signal represents a secondary conformational rearrangement which occurs to stabilize the preformed polymer. This structural rearrangement may be the conformational change that has been postulated to occur in tubulin prior to GTP hydrolysis (Carlier & Pantaloni, 1981), a phenomenon that also displays a kinetic profile distinct from the light scattering observed during microtubule formation.

References

Baker, T. S., & Amos, L. A. (1978) *J. Mol. Biol. 123*, 89–106.

Bhattacharya, B., & Wolff, J. (1974) *Proc. Natl. Acad. Sci. U.S.A. 71*, 2627–2631.

Bhattacharya, B., & Wolff, J. (1984) *J. Biol. Chem. 259*, 11836–11843.

Bonne, D., Heusèle, C., Simon, C., & Pantaloni, D. (1985) *J. Biol. Chem. 260*, 2819–2825.

Bordas, J., Mandelkow, E.-M., & Mandelkow, E. (1983) *J. Mol. Biol. 164*, 89–135.

Borisy, G. G., Marcum, J. M., Olmsted, J. B., Murphy, D. B., & Johnson, K. A. (1975) *Ann. N.Y. Acad. Sci. 253*, 107–132.

Burton, P. R. (1981) *Cell Muscle Motil. 1*, 289–333.

Carlier, M.-F., & Pantaloni, D. (1978) *Biochemistry 17*, 1908–1915.

Carlier, M.-F., & Pantaloni, D. (1981) *Biochemistry 20*, 1918–1924.

Ceska, T. A., & Edelstein, S. J. (1984) *J. Mol. Biol. 175*, 349–370.

Clark, D. C., Marten, S. R., & Bayley, P. M. (1981) *Biochemistry 20*, 1924–1932.

Correia, J. J., & Williams, R. C. (1983) *Annu. Rev. Biophys. Bioeng. 12*, 211–235.

Correia, J. J., & Williams, R. C. (1985) *Arch. Biochem. Biophys. 239*, 120–129.

Detrich, H. W., & Williams, R. C. (1978) *Biochemistry 17*, 3900–3907.

Dustin, P. (1984) *Microtubules*, 2nd ed., Springer-Verlag, Berlin.

Dustin, P., Flament-Durant, J., Couch, A. M., & Depierreaux, M. (1980) *J. Submicros. Cytol. 12*, 611–616.

Eagle, G. R., Zombola, R. R., & Himes, R. H. (1983) *Biochemistry 22*, 221–228.

Erickson, H. P., & Pantaloni, D. (1981) *Biophys. J. 34*, 293–310.

Förster, Th., & Hoffmann, G. (1971) *Z. Phys. Chem. (Weisbaden) 75*, 63–76.

Frigon, R. P., & Timasheff, S. N. (1975) *Biochemistry 14*, 4559–4566.

Gaskin, F., & Kress, Y. (1977) *J. Biol. Chem. 252*, 6918–6924.

Gaskin, F., Cantor, C. R., & Shelanksi, M. (1974) *J. Mol. Biol. 119*, 737–758.

Horowitz, P. M., & Criscimagna, N. L. (1985) *Biochemistry 24*, 2587–2593.

Horowitz, P., Prasad, V., & Luduena, R. F. (1984) *J. Biol. Chem. 259*, 14647–14650.

Kirschner, M. W. (1978) *Int. Rev. Cytol. 54*, 1–71.

Kravit, N. G., Regula, C. S., & Berlin, R. D. (1984) *J. Cell Biol. 99*, 188–198.

Kuder, J. E., Limberg, W. W., Pochan, J. M., & Wychick, D. (1977) *J. Chem. Soc., Perkins Trans. 2*, 1643–1651.

Kung, C. E., & Reed, J. K. (1986) *Biochemistry 25*, 6114–6121.

Lakowicz, J. R. (1983) in *Principles of Fluorescence Spectroscopy*, p 44, Plenum Press, New York.

Loutfy, R. O. (1981) *Macromolecules 14*, 270–275.

Loutfy, R. O. (1986) *Pure Appl. Chem. 58*, 1239–1248.

Loutfy, R. O., & Law, K. Y. (1980) *J. Phys. Chem. 84*, 2803–2808.

Loutfy, R. O., & Arnold, B. A. (1982) *J. Phys. Chem. 86*, 4205–4211.

Lowry, O. H., Rosebrough, N. J., Farr, A. L., & Randall, R. J. (1951) *J. Biol. Chem. 252*, 6222–6228.

Mandelkow, E., & Mandelkow, E.-M. (1981) *J. Ultrastruct. Res. 74*, 11–33.

Mandelkow, E., Mandelkow, E.-M., & Bordas, J. (1983) *Trends Biochem. Sci. (Pers. Ed.) 8*, 374–377.

Mandelkow, E.-M., Harmon, A., Mandelkow, E., & Bordas, J. (1980) *Nature 287*, 595–599.

Marcum, J. M., & Borisy, G. G. (1978) *J. Biol. Chem. 253*, 2825–2833.

McEwen, B. F., Ceska, T. A., Crepeau, R. H., & Edelstein, S. J. (1983) *J. Mol. Biol. 166*, 119–140.

Munson, P. J., & Robbard, D. (1980) *Anal. Biochem. 107*, 220–239.

Murphy, D. (1982) *Methods Cell Biol. 24*, 31–49.

Murphy, D. B., & Borisy, G. G. (1972) *Proc. Natl. Acad. Sci. U.S.A. 72*, 2696–2700.

Roberts, K., & Hyams, J. S., Eds. (1979) *Microtubules*, Academic Press, London.

Schultheiss, R., & Mandelkow, E. (1983) *J. Mol. Biol. 170*, 471–496.

Spann, U., Renna, W., Mandelkow, E.-M., Bordas, J., & Mandelkow, E. (1987) *Biochemistry 26*, 1123–1132.
Tamm, L. K., Crepeau, R. H., & Edelstein, S. J. (1979) *J. Mol. Biol. 130*, 473–493.
Vallee, R. B., & Borisy, G. G. (1978) *J. Biol. Chem. 253*, 2834–2845.
Wang, J. L., & Edelman, G. M. (1971) *J. Biol. Chem. 246*, 1185–1191.
White, E. A., Burton, P. R., & Himes, R. H. (1987) *Cell Motil. Cytoskel. 7*, 31–38.
Williams, R. C., & Detrich, H. W. (1979) *Biochemistry 18*, 2499–2503.

Molecular Basis of the Heat Denaturation of Photosystem II†

Lynmarie K. Thompson, Richard Blaylock, Julian M. Sturtevant, and Gary W. Brudvig*
Department of Chemistry, Yale University, New Haven, Connecticut 06511
Received December 19, 1988; Revised Manuscript Received April 27, 1989

ABSTRACT: The thermal denaturation of the photosystem II (PSII) membrane protein complex is investigated by assigning the endothermic transitions observed by differential scanning calorimetry (DSC) to the denaturation of particular proteins of the PSII complex. In a prior DSC study of PSII membranes [Thompson, L. K., Sturtevant, J. M., & Brudvig, G. W. (1986) *Biochemistry 25*, 6161], five DSC peaks were observed in the 30–70 °C temperature range (A_1, A_2, B, C, and D). The A_2 peak was assigned to denaturation of a component essential for water oxidation and the B peak to denaturation of a component critical to the remainder of the electron-transport chain. We have now extended these studies with thermal gel analysis and electron paramagnetic resonance (EPR) measurements. Thermal gel analysis, a technique which relies on a change in the solubility properties of a membrane protein upon denaturation, has been used to determine the temperatures of denaturation of all of the major membrane proteins of the PSII complex. EPR experiments have been used to monitor chlorophyll photooxidation and the stability of Tyr_{D^+}. Peaks B, C, and D in the DSC denaturation profile are each assigned to the denaturaation of several proteins, which provides information on the organization of the PSII complex into structural and functional units. Peak B corresponds to the denaturation of peripheral core proteins and closely associated antenna proteins, peak C to the PSII core, and peak D to the loosely associated antenna proteins. No membrane protein is observed to denature during the A_2 peak. The A_2 peak is altered by the presence of catalase, superoxide dismutase, low chloride, and high pH. These results suggest that the abnormally sharp A_2 peak occurs when the highly oxidizing, sequestered Mn complex (the active site in water oxidation) becomes accessible to the aqueous phase, at elevated temperatures. We propose a mechanism for the reaction of the Mn complex with hydroxide ions, which involves peroxide or superoxide and results in the reduction and release of Mn. The proposed model provides insight into the well-known instability of the Mn complex and the role of chloride in stabilizing the complex. This may enable the future development of purification procedures and may explain the sensitivity of the water-oxidizing apparatus of PSII to heat denaturation.

Photosystem II (PSII)[1] is a multicomponent membrane protein complex which utilizes light energy to drive uphill electron-transport reactions and oxidize water. The water oxidation reaction, which occurs at an active site composed of four Mn ions, is the most heat-sensitive component of the entire photosynthetic electron-transport chain (Katoh & San Pietro, 1967). We have used differential scanning calorimetry (DSC) in combination with other techniques to investigate the heat denaturation of PSII, in order to provide insight into the structural organization of the complex and the individual roles of the component proteins, as well as to determine the molecular basis of the heat sensitivity of the water-oxidizing apparatus.

PSII utilizes a photon of light absorbed by P680, the special Chl primary electron donor, to catalyze electron transfer from water to plastoquinone:

$$H_2O \rightarrow \text{Mn complex} \rightarrow Tyr_Z \rightarrow P680 \rightarrow \text{pheophytin} \rightarrow Q_A \rightarrow Q_B$$

Components prior to P680 in this main electron-transfer chain

†This work was supported by the National Institutes of Health (GM32715) and the Herman Frasch Foundation. G.W.B. is the recipient of a Camille and Henry Dreyfus Teacher/Scholar award and an Alfred P. Sloan Foundation research fellowship. L.K.T. is the recipient of a dissertation fellowship from the American Association of University Women.

[1] Abbreviations: Chl, chlorophyll; DCBQ, 2,5-dichloro-*p*-benzoquinone; DCIP, 2,6-dichlorophenolindophenol; DCMU, 3-(3,4-dichlorophenyl)-1,1-dimethylurea; DPC, *sym*-diphenylcarbazide; DSC, differential scanning calorimetry; EPR, electron paramagnetic resonance; HEPES, *N*-(2-hydroxyethyl)piperazine-*N*′-2-ethanesulfonic acid; kDa, kilodalton(s); LHCP, light-harvesting chlorophyll *a*/*b* protein(s); MES, 2-(*N*-morpholino)ethanesulfonic acid; OGP, octyl glucopyranoside; PSII, photosystem II; P680, primary electron donor in PSII; Q_A, primary quinone electron acceptor in PSII (bound plastoquinone); Q_B, secondary quinone electron acceptor in PSII (plastoquinone binding site); SDS–PAGE, sodium dodecyl sulfate–polyacrylamide gel electrophoresis; Tris, tris(hydroxymethyl)aminomethane; Tyr_D, a Tyr residue which upon photooxidation gives rise to a dark-stable radical EPR signal; Tyr_Z, a Tyr residue which functions as the secondary electron donor in PSII; TX-100, Triton X-100.

0006-2960/89/0428-6686$01.50/0 © 1989 American Chemical Society